CARD10 promotes the progression of renal cell carcinoma by regulating the NF-κB signaling pathway

LONGFEI PENG[*], KE HE[*], ZHANGJUN CAO[*], LIANGKUAN BI, DEXIN YU, QI WANG and JINYOU WANG

Department of Urology, The Second Affiliated Hospital of Anhui Medical University, Hefei, Anhui 230032, P.R. China

Abstract. Previous studies have demonstrated that the expression of CARD10 is closely associated with the occurrence of tumors, and its role is mainly to promote tumor progression by activating the transcription factor NF-κB. However, the signaling pathway in renal cancer remains unclear. The objective of the present study was to investigate the ability of caspase recruitment domain 10 (CARD10) to regulate the NF-κB signaling pathway and promote the progression of renal cell carcinoma (RCC). Expression of CARD10 in ACHN, 786-O and HK-2 cells was evaluated via western blot analysis, as was the epidermal growth factor (EGF)-induced activation of NF-κB signaling pathway-related proteins in cells. The expression of CARD10 was inhibited by CARD10 short hairpin RNA transfection. Cell cycle analysis and MTT assays were used to evaluate cell proliferation. Cell apoptosis was analyzed via flow cytometry. The invasion of renal cell lines was detected via Transwell cell migration and invasion assays *in vitro*. The results showed that CARD10 expression was significantly higher in RCC cells than in normal renal tubular epithelial cells. CARD10 silencing inhibited the proliferation, invasion and migration of RCC cells. EGF stimulation upregulated the activation of the NF-κB pathway in RCC cells. Inhibition of CARD10 expression inhibited NF-κB activation in RCC cells. Taken together, these data suggested that CARD10 promotes the progression of renal cell carcinoma by regulating the NF-κB signaling pathway. Thus, this indicated that CARD10 may be a novel therapeutic target in RCC.

Correspondence to: Professor Liangkuan Bi, Department of Urology, The Second Affiliated Hospital of Anhui Medical University, 678 Hibiscus Road, Hefei, Anhui 230032, P.R. China
E-mail: plofei@126.com

[*]Contributed equally

Introduction

Renal cell carcinoma (RCC) is the second most common malignant tumor of the urinary system, with an incidence that is increasing annually. RCC is associated with >140,000 deaths per year. The incidence of RCC is more prominent in men, with a male-to-female ratio of 1.5:1, and peaks at age 60-70 years (1). Early clinical manifestations of RCC are not easily detectable, and 1/4-1/3 of patients have metastasis at the time of clinical diagnosis (2,3). Therefore, the treatment of RCC is highly challenging. The caspase recruitment domain (CARD) protein family has three main members, known as CARD10, CARD11 and CARD14. CARD11 is expressed mainly in lymphatic tissues, as well as certain hematopoietic organs, including the spleen and thymus. CARD14 is expressed mainly in the skin and mucous membranes (4,5). CARD10, also known as CARMA3 (6), is widely distributed in all non-hematopoietic tissues, such as the heart, kidney and liver (6-9). High expression of CARD10 has also been found in a variety of solid tumors, such as colorectal (10), lung (11), pancreatic (12), breast (13), ovarian (14), renal (15) and bladder cancers (16,17). In colon, lung, pancreatic and breast cancers, studies have shown that CARD10 promotes growth and invasion of tumor cells, and inhibits apoptosis (10-13). Furthermore, increased expression of CARD10 is closely related to malignancy (18-20). CARD10 exerts its biological functions mainly through the NF-κB signaling pathway (7,21,22). This is via a mechanism predominantly involved in the regulation of the IκB kinase complex by the CARD11-B-cell lymphoma 10 (BCL10)-mucosa-associated lymphoid tissue lymphoma gene 1 (MALT1) complex, which is composed of downstream BCL10 and MALT1 (7,21,22). However, the mechanism by which CARD10 modulates signaling pathways that promote RCC invasion and migration remains unclear. Therefore, this study investigated the ability of CARD10 to regulate the NF-κB signaling pathway and promote disease progression in RCC. This information may provide a novel therapeutic target in RCC.

Materials and methods

Materials. Human RCC cell lines (ACHN and 786-O) and the human renal tubular epithelial cell line HK-2 were purchased from The Cell Bank of Type Culture Preservation Committee of the Chinese Academy of Sciences. Transfection vectors

[short hairpin (sh)GFP and shCARD10] were purchased from Shanghai GeneChem Co., Ltd. Anti-CARD10 antibody (cat. no. ab36839), anti-IκBα antibody (cat. no. ab32518), anti-p-65 antibody (cat. no. ab32536), anti-phosphorylated (p)-p-65 antibody (cat. no. ab86299), anti-β-actin antibody (cat. no. ab8226), goat anti-rabbit IgG (cat. no. ab6721) and goat anti-rat IgG (cat. no. ab97057) were purchased from Abcam. Modified Eagle's Media (MEM), Roswell Park Memorial Institute (RPMI) 1640 medium, Dulbecco's Modified Eagle's Medium: Nutrient Mixture F-12 (DMEM/F12) and fetal bovine serum (FBS) were purchased from Gibco (Thermo Fisher Scientific, Inc.). The MTT cell proliferation, and cell cycle and apoptosis analysis kits were purchased from BestBio. Transwell chambers and Matrigel matrix were purchased from Corning Life Sciences. SDS-PAGE gel preparation kit, ECL photoluminescence kit, pancreatic cell digestion solution, bicinchoninic acid (BCA) protein assay kit and PBS were purchased from Beyotime Institute of Biotechnology.

Cell culture. ACHN, 786-O and HK-2 cells were cultured in MEM, RPMI 1640 and DMEM/F12 medium, respectively, supplemented with 10% FBS at 37°C under 5% CO_2.

Western blot analysis. Total cellular proteins were extracted using a 100:1 mixed solution of RIPA buffer (Beyotime Institute of Biotechnology) and PMSF (Beyotime Institute of Biotechnology.). The protein concentrations were measured using a BCA Protein Assay kit. Target proteins (30 μg) were separated via SDS-PAGE on a 10% gel and transferred to PVDF membranes. Non-specific binding was blocked by incubation in 5% non-fat dried milk for 2 h at room temperature. Membranes were then incubated overnight at 4°C with primary antibodies (dilutions: CARD10, 1:200; IκBα, 1:5,000; NF-κB p65, 1:1,000; p-NF-κB p65, 1:1,000). After washing, the membranes were then incubated with the appropriate HRP-conjugated secondary antibodies (dilution: 1:10,000) at room temperature for 2 h. Finally, after washing, immunoreactive protein bands were detected using an ECL kit and quantified using ImageJ Pro Plus 6.0 software (National Institutes of Health).

CARD10 shRNA transfection. Cultured RCC cells (ACHN and 786-O; ~90% confluent) were seeded (2.5x10⁵/ml) in 24-well tissue culture plates (Beyotime Institute of Biotechnology). Subsequently, when the cell confluency was ~60%, 20 pmol CARD10 shRNA (or shGFP as the negative control) was dissolved in 50 μl Opti-MEM (HyClone; GE Healthcare Life Sciences, and 1 μl Lipofectamine® 2000 reagent (Thermo Fisher Scientific, Inc.) was dissolved in 50 μl Opti-MEM before both solutions were mixed at room temperature for 5 min. Finally, at ~90% confluence, the culture medium was replaced with 400 μl serum-free medium and 100 μl transfection mixture was added. Cells were incubated for 4-6 h before the transfection medium was replaced with complete medium. After cultivation for 24-48 h, proteins were extracted and successful transfection was confirmed via western blot analysis.

Transwell cell migration and invasion assays. For Transwell invasion assays, 100 μl Matrigel (1 mg/ml) was added vertically to the membrane in the Transwell upper chamber and incubated at 37°C for 4-5 h until dry. The basement membrane was hydrated by incubation with serum-free medium at 37°C. Medium (600-800 μl) containing 10% FBS was added in the lower chamber and 100-150 μl cell suspension (2x10⁵/ml) was added to the upper chamber. Plates were incubated at 37°C for 24 h before cells that had invaded the Matrigel were fixed with 4% paraformaldehyde for 30 min at room temperature, stained with 0.5% crystal violet solution for 15-30 min at room temperature and counted under an inverted light microscope (Olympus Corporation; CKX31; magnification, x100).

For Transwell migration assays, the cell suspension was prepared as described previously. Medium (600-800 μl) containing 10% FBS was added in the lower chamber and 100-200 μl cell suspension (3x10⁵/ml) was added to the upper chamber. Plates were incubated at 37°C for 36 h before cells that had migrated from the upper chamber to the lower chamber were fixed with 4% paraformaldehyde for 20 min at room temperature, stained with 0.5% crystal violet for 30 min at room temperature and counted under an inverted light microscope (Olympus Corporation; CKX31; magnification, x100).

Cell cycle analysis. Cells cultured in 6-well tissue culture plates were washed and resuspended with 0.5 ml pre-cooled PBS. Cells were then fixed by the addition of 1.2 ml pre-cooled anhydrous ethanol (final ethanol concentration was 70%) at -20°C for 1 h. Fixed cells were harvested by centrifugation at 3,600 x g for 10 min at room temperature. After removing the supernatant, cells were washed twice with 1.8 ml PBS and centrifuged at 600 x g at room temperature. The supernatant was discarded, and the cells were resuspended in 100 μl RNase-A (50 μg/ml), mixed and digested at 37°C for 30 min. Nuclei were stained with 100 μl propidium iodide (PI) dye solution (final concentration 50 μg/ml) at 4°C in the dark for 30 min. Flow cytometric analysis (NAVIOS; Beckman Coulter, Inc.) of ~3x10⁴ cells was performed immediately using MultiCycle software version 10.1 (Phoenix Flow Systems, Inc.).

MTT assay. Cells were seeded into 96-well flat-bottomed tissue culture plates (5-10x10³/well in 100 μl medium). The cells were cultured for 24-96 h at 37°C under 5% CO_2 before the addition of 10 μl/well MTT solution (5 mg/ml, 0.5% MTT). Cells were cultured for a further 4 h before the addition of 150 μl dimethyl sulfoxide to dissolve crystals. Cell proliferation was measured at 490 nm by an ELISA plate reader.

Cell apoptosis analysis. Cells (0.5-1x10⁶) were centrifuged at 800 x g for 3 min at room temperature. After washing twice with pre-cooled PBS, cells were resuspended with 100 μl 1X binding buffer (BestBio) and 5X allophycocyanin conjugated to Annexin V was added. After incubation for 15 min at room temperature, 10 μl PI was added and the cells were incubated at room temperature in the dark for 5 min. Flow cytometric analysis (NAVIOS) of ~3x10⁶ cells was performed immediately using Kaluza 2.0 software (Beckman Coulter, Inc.).

Activation of NF-κB. The cell suspension (786-O and ACHN cells) was prepared and inoculated into four Petri dishes at 37°C under 5% CO_2. When the cell density was ~90%,
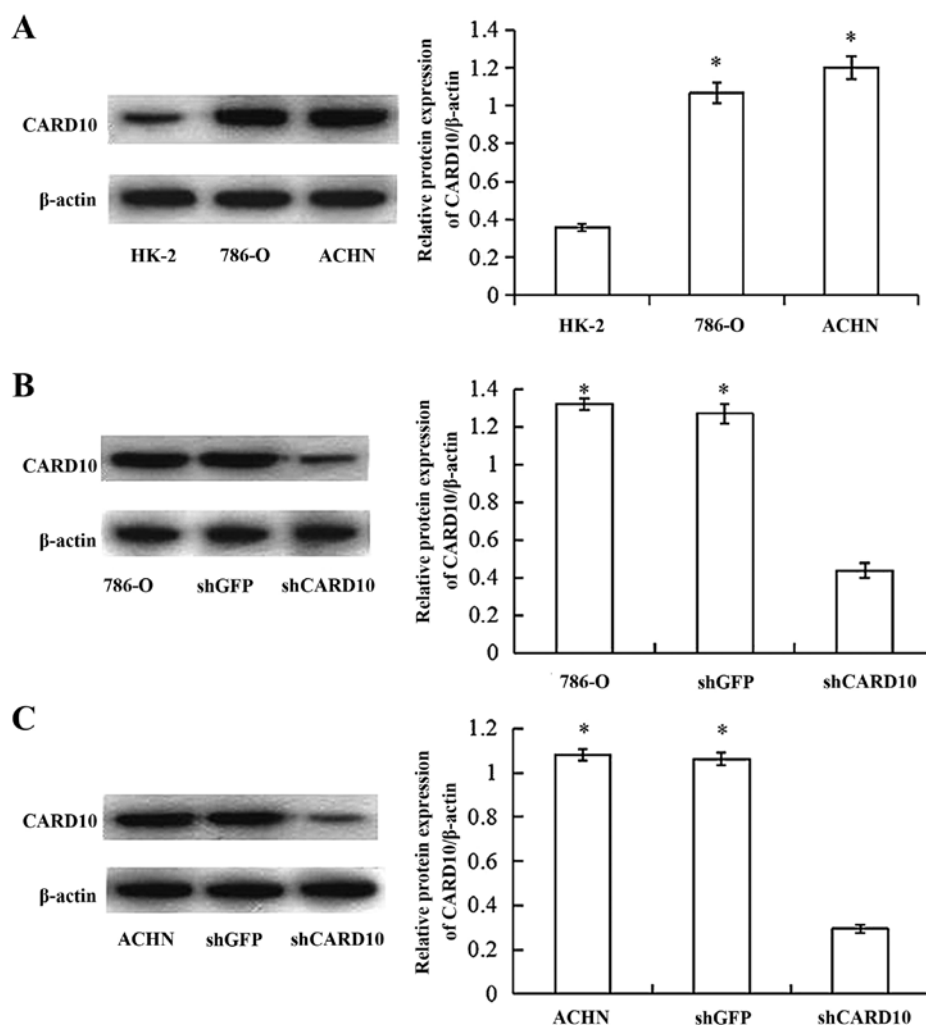
Figure 1. Expression of CARD10 in RCC cells compared with in normal renal tubular epithelial cells. (A) Western blot analysis detected a higher CARD10 content in the 786-O and ACHN RCC cells than in HK-2 cells. *P<0.05 vs. HK-2. After the transfection of (B) 786-O and (C) ACHN RCC cells for 48 h, western blot analysis was performed. *P<0.05 vs. shCARD10. CARD10, caspase recruitment domain 10; RCC, renal cell carcinoma; sh, short hairpin (RNA).

EGF (AF-100-15; PeproTech, Inc.) was added into the four Petri dishes and the concentration was adjusted to 10 ng/ml. The cells were treated for 0, 7.5, 15 and 30 min. shGFP and shCARD10 cell lines (786-O and ACHN cells) were established by transfecting cells with shRNA. EGF was added to three plates, and the concentration was adjusted to 10 ng/m. The cells were treated for 0, 15 and 30 min. The treatment of HK-2, 786-O and ACHN cells was the same as before.

Statistical analysis. Data are presented as the mean ± SD. The statistical analysis was performed using SPSS version 19.0 (IBM, Corp.). Comparisons were performed with Student's t-test. Statistical differences among multiple groups were analyzed by one-way ANOVA and Tukey's post hoc test. P<0.05 was considered to indicate a statistically significant difference. Each experiment was repeated at least three times.

Results

High expression of CARD10 in RCC cells. Western blot analysis confirmed that the expression of CARD10 in RCC cells (786-O and ACHN) was significantly higher compared with in normal renal tubular epithelial cells (HK-2; P<0.05; Fig. 1A).

CARD10 promotes the growth of RCC cells. After 48 h of transfection, the total protein of the cells was extracted and the effect of transfection was verified via western blot analysis. CARD10 protein expression was significantly decreased in cells transfected with CARD10 shRNA (P<0.05; Fig. 1B and C). The effects of shRNA-mediated CARD10 silencing on RCC function were investigated. At 48 h after transfection, MTT assays showed that cell proliferation in the 786-O-shCARD10 group was significantly lower than that in the 786-O and 786-O-shGFP groups (P<0.05; Fig. 2A). However, there were no significant differences in the cell proliferation ability between the 786-O and 786-O-shGFP groups (Fig. 2A). Furthermore, flow cytometric analysis of the cell cycle distribution in the three groups showed a higher proportion of G1 phase cells in the 786-O-shCARD10 group compared with the other two groups, while the proportion of S phase cells was significantly reduced (P<0.05; Fig. 3A and C). To confirm that CARD10 promoted RCC growth, apoptosis in the three groups of cells was also analyzed. The percentage of apoptotic cells
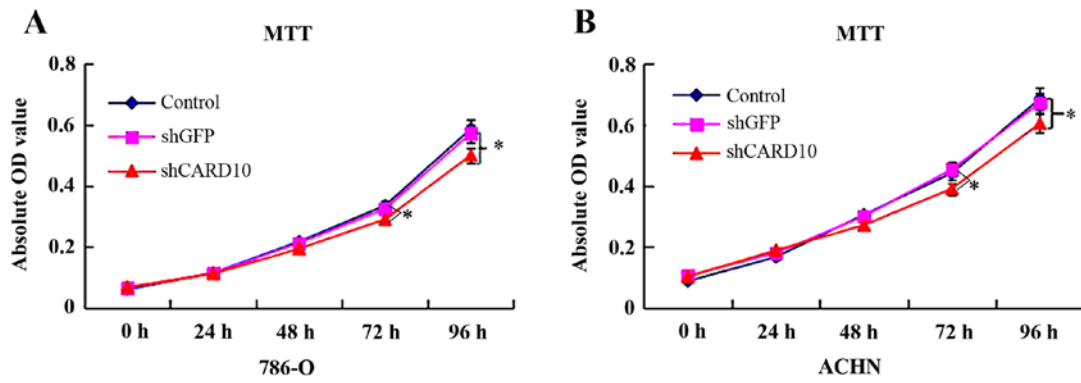
Figure 2. CARD10 knockdown reduces the proliferative ability of renal cell carcinoma cells. (A) After 786-O cell transfection, proliferation was analyzed at 0, 24, 48, 72 and 96 h by MTT assays. The results show that after transfection for 48 h, the 786-O-shCARD10 group exhibits significantly reduced proliferative ability compared with the other two groups of cells, and the difference gradually increased with time. (B) ACHN cells showed the same results. *P<0.05. CARD10, caspase recruitment domain 10; sh, short hairpin (RNA); OD, optical density.
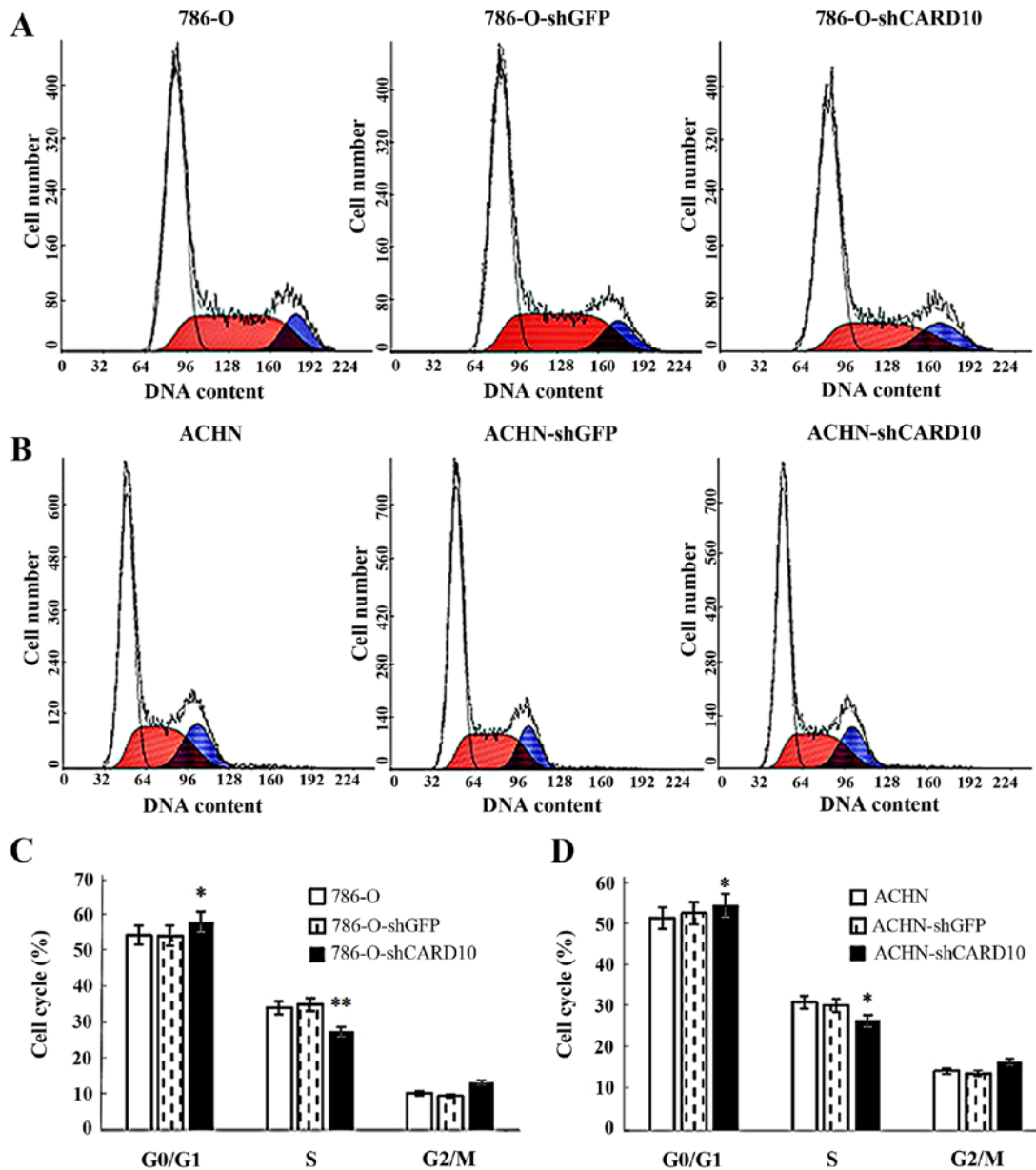

Figure 3. Cell cycle arrest in renal cell carcinoma cells after CARD10 knockdown. Stages of the cell cycle of (A) 786-O, 786-O-shGFP and 786-O-shCARD10 and (B) ACHN, ACHN-shGFP and ACHN-shCARD10. (C) 786-O-shCARD10 group compared with the other two groups had a higher proportion of G1 phase cells, and a reduced proportion of S phase cells. *P<0.05, **P<0.01 vs. 786-O. (D) ACHN-shCARD10 group compared with the other two groups had a higher proportion of G1 phase cells, and a reduced proportion of S phase cells. *P<0.05 vs. ACHN. CARD10, caspase recruitment domain 10; sh, short hairpin (RNA).
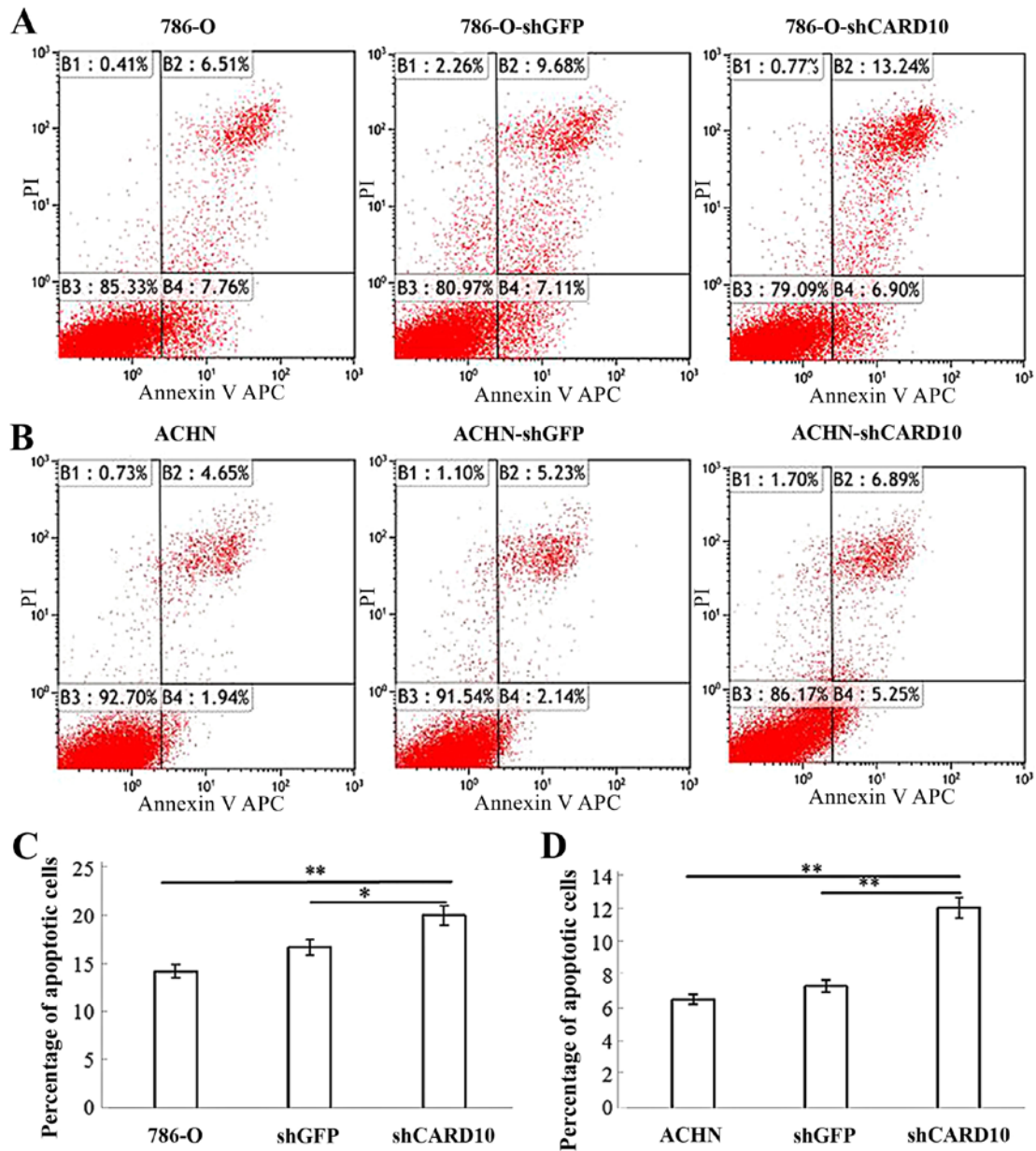
Figure 4. Increased apoptosis of renal cell carcinoma cells after CARD10 knockdown. (A) Distribution of apoptosis in 786-O, 786-O-shGFP and 786-O-shCARD10 cells. (B) Distribution of apoptosis in ACHN, ACHN-shGFP and ACHN-shCARD10 cells. (C) Following shCARD10 transfection, the percentage of apoptotic cells in the 786-O-shCARD10 group was significantly higher than that in the other two groups. (D) Similar results were obtained for the ACHN-shCARD10 group. *P<0.05, **P<0.01, as indicated. CARD10, caspase recruitment domain 10; sh, short hairpin (RNA); PI, propidium iodide; APC, allophyocyanin.

in the 786-O-shCARD10 group was significantly higher than that in the other two groups (P<0.05; Fig. 4A and C). Similar results for these three experiments were obtained in ACHN cells (Figs. 2B, 3B and D, and 4B and D). Therefore, it can be concluded that CARD10 promotes growth and inhibits apoptosis in RCC cells.

CARD10 promotes the invasion of RCC cells. To further examine whether CARD10 contributes to the migration and invasion of RCC cells, migration and Matrigel invasion assays in Transwell chambers were performed. In invasion assays, the number of cells passing through the Matrigel in the 786-O-shCARD10 group was significantly reduced compared with in the 786-O and 786-O-shGFP groups, with relative

inhibition rates of 57±10.6 and 51.4±12.6%, respectively, after 48 h (P<0.05; Fig. 5A and C). In migration assays, the number of cells that migrated from the upper chamber to the lower chamber in the Transwell plates was significantly lower in the 786-O-shCARD10 group compared with that in the 786-O and 786-O-shGFP groups, with inhibition rates of 62.3±5.6 and 55.2±7.3%, respectively, at 48 h (P<0.05; Fig. 5A and D). Similarly, the number of cells passing through the Matrigel in the ACHN-shCARD10 group was significantly reduced compared to that in the ACHN and ACHN-shGFP groups, with inhibition rates of 47.5±4.1 and 30.9±4.5%, respectively, at 48 h (P<0.05; Fig. 5B and E). Furthermore, the number of cells that migrated from the upper chamber to the lower chamber in the Transwell plates in the ACHN-shCARD10
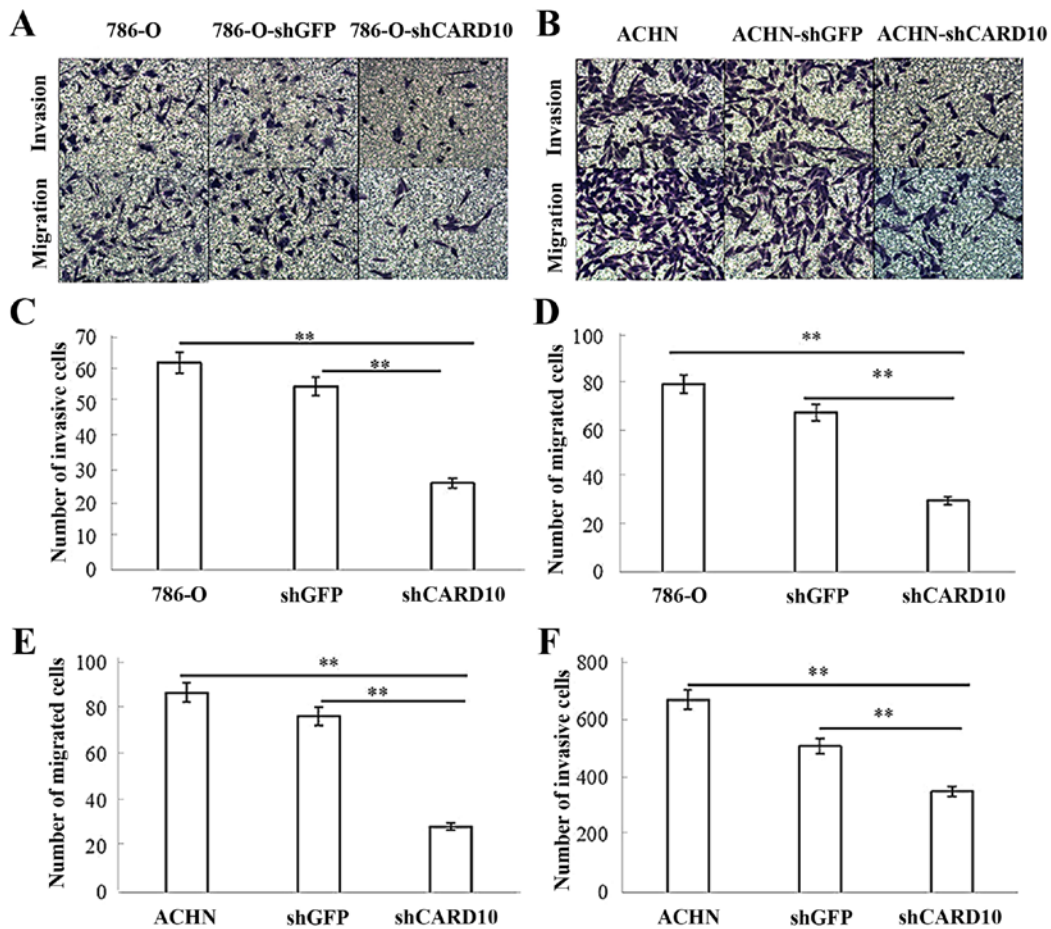
Figure 5. Invasive and migratory abilities of RCC cells are reduced after CARD10 knockdown. (A) Invasion and migration of 786-O-shCARD10 group RCC cells was were decreased. (B) Invasion and migration of ACHN-shCARD10 group RCC cells were decreased. Magnification, x100. (C) Compared with the other two groups, the number of migratory 786-O-shCARD10 cells decreased significantly. (D) Compared with the other two groups, the number of migratory ACHN-shCARD10 cells decreased significantly. (E) Compared with the other two groups, the number of invasive 786-O-shCARD10 cells decreased significantly. (F) Compared with the other two groups, the number of invasive ACHN-shCARD10 cells decreased significantly. The bar graph indicates the mean ± SD of cells per imaged frame, calculated from the average number of cells in ten fields. **P<0.01. CARD10, caspase recruitment domain 10; RCC, renal cell carcinoma; sh, short hairpin (RNA).

group was significantly reduced compared with that in the ACHN and ACHN-shGFP groups, with inhibition rates of 62.3±5.6 and 55.2±7.3%, respectively, at 48 h (P<0.05; Fig. 5B and F).

CARD10 knockdown inhibits activation of the NF-κB signaling pathway in RCC cells. To investigate the mechanism by which CARD10 promoted the progression of RCC, the effect of CARD10-knockdown on IκBα, NF-κB p65 and p-p65 levels was tested. First, 786-0 cells were stimulated with epidermal growth factor (EGF; 10 ng/ml) for 0, 7.5, 15 and 30 min. The expression of proteins related to activation of the NF-κB signaling pathway was then evaluated via western blot analysis. IκBα protein expression decreased significantly in a time-dependent manner, while the p-p65/p65 content increased (P<0.05; Fig. 6A). These results demonstrated that EGF stimulated activation of the NF-κB signaling pathways in RCC cells. Then, 786-O-shGFP and 786-O-shCARD10 cells were treated with EGF (10 ng/ml) for 0, 15 and 30 min; 786-O-shGFP cells were used as a negative control group. Western blot analysis showed that there was a significantly higher

IκBα protein content and lower p-p65/p65 content in the 786-O-shCARD10 group compared with that in the negative control group when measured at the same time point (P<0.05; Fig. 6B). These results demonstrated that CARD10 knockdown inhibited the activation of the NF-κB signaling pathway-related proteins in 786-0 cells. Similar results were obtained when the experiments were repeated with ACHN cells (Fig. 6C and D). NF-κB activation in HK-2 cells and RCC cells was further validated following prolonged EGF (10 ng/ml) treatment. The results showed significantly higher IκBα protein content and decreased p65 phosphorylation in HK-2 cells than that in the RCC cells when measured at the same time point (P<0.05; Fig. 6E).

Discussion

A previous study in the literature demonstrated that CARD10 expression in RCC is significantly higher than that in adjacent non-cancerous tissues (15). In the present study, it was first verified that CARD10 was expressed at higher levels in RCC cells than in normal renal tubular epithelial cells. Secondly, because CARD10 has been found to promote the growth
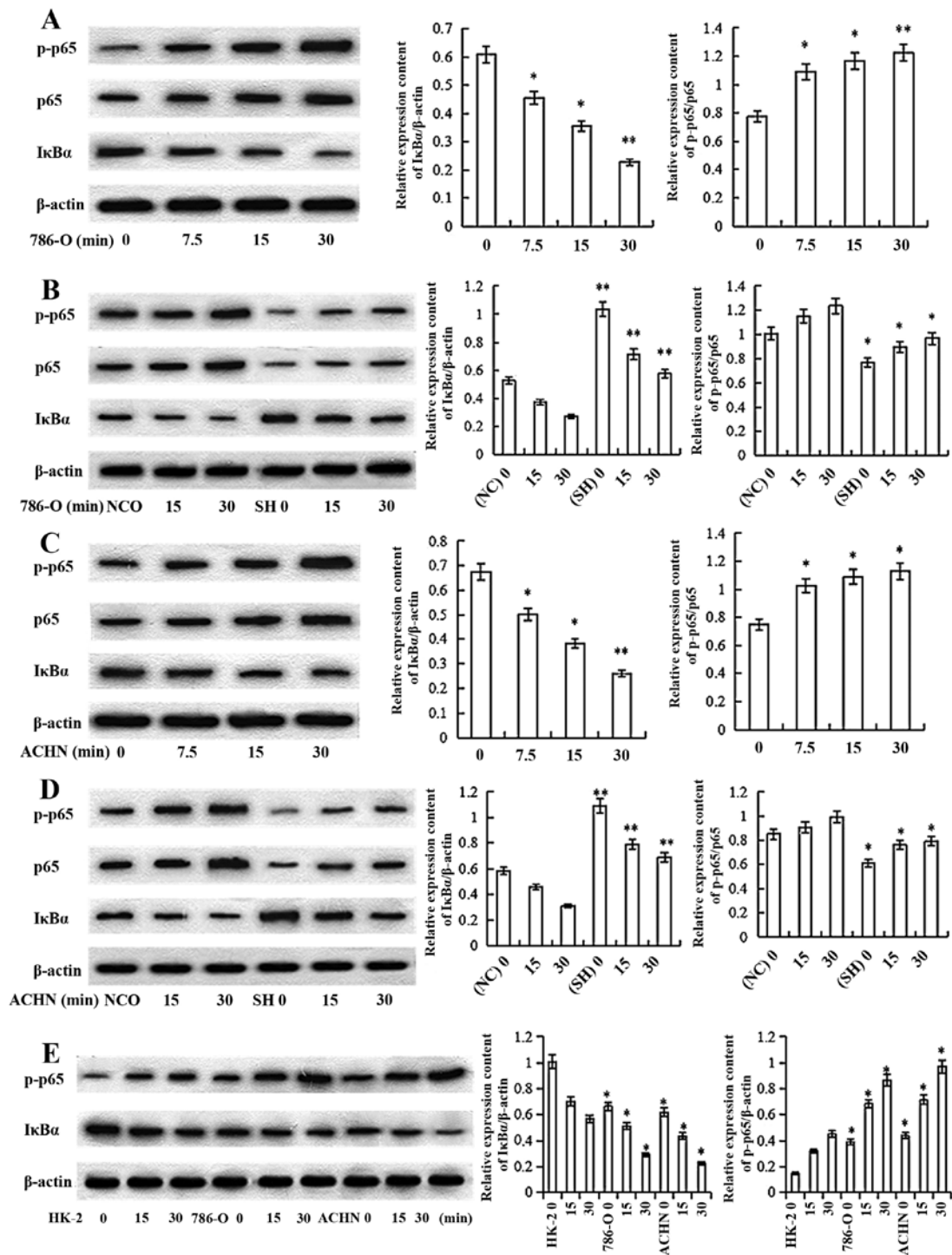
Figure 6. Inhibiting the expression of CARD10 can inhibit the activation of NF-κB signaling pathways in RCC. (A) 786-0 cells were stimulated with EGF (10 ng/ml) for 0, 7.5, 15 and 30 min. With the prolongation of treatment time, IκBα levels were increasingly downregulated, while p-p65/p65 content showed an upward trend. *P<0.05, **P<0.01 vs. 0 ng/ml. (B) 786-O NC (shGFP transfection) group and the experimental group (shCARD transfection) were treated with EGF (10 ng/ml) for 0, 15 and 30 min. At the same treatment time, the experimental group had higher IκBα protein content and lower p-p65/p65 content than the negative control group. The bar graph indicates relative expression of various proteins. *P<0.05, **P<0.01 vs. NC. (C) ACHN cell were stimulated with EGF (10 ng/ml) for 0, 7.5, 15 and 30 min. With the prolongation of treatment time, IκBα levels were increasingly downregulated, while p-p65/p65 content showed an upward trend. *P<0.05, **P<0.01 vs. 0 ng/ml. (D) ACHN NC (shGFP transfection) group and the experimental group (shCARD transfection) were treated with EGF (10 ng/ml) for 0, 15 and 30 min. At the same treatment time, the experimental group had higher IκBα protein content and lower p-p65/p65 content than the negative control group. The bar graph indicates relative expression of various proteins. *P<0.05, **P<0.01 vs. NC. (E) Normal HK-2 cells and RCC cell lines were treated with EGF (10 ng/ml) for 0, 15 and 30 min. At the same treatment time, there was significantly higher IκBα protein content and lower p-p65 content in HK-2 cells than in the RCC cells. *P<0.05 vs. HK-2. CARD10, caspase recruitment domain 10; EGF, epidermal growth factor; NC, negative control; p, phosphorylated; RCC, renal cell carcinoma; sh, short hairpin (RNA).

of a variety of types of tumors, such as rectal (10), lung (11), and breast cancer (13), the aim was to verify the involvement

of CARD10 in the proliferation and invasion of RCC. The ACHN and 786-O renal cancer cell lines were transfected

with CARD10 shRNA to silence CARD10 expression. Finally, the proliferative, invasive and migratory abilities of RCC cell lines were examined after transfection with CARD10 shRNA compared with a negative control. These results showed that CARD10 promoted proliferation and invasion in two different RCC cell lines.

NF-κB, which is a protein with multiple transcriptional regulatory functions, participates in the transcriptional regulation of genes related to inflammation, stress response, immune cell activation, proliferation, differentiation, apoptosis and tumorigenesis (23,24). NF-κB is activated via classical and non-classical pathways, although the classical pathway is more common (24). In the stationary state, NF-κB exists in the cell cytoplasm in the inactive state combined with the inhibitor IκB to form a trimer p50-p65-IκB. Following activation, IκB is released from the p50-p65-IκB timer to form a p50-p65 dimer (25-27). Studies have shown that guanosine-binding protein-coupled receptor (28), EGF receptor (28-30) and protein kinase C (31) induce NF-κB activation (32). EGF consists of 53 amino acids and is characterized by its ability to promote cell proliferation. EGF is the prototypical growth-promoting cytokine, but also has well-established roles in stimulating tumor-initiating stem cells and tumorigenesis (33). EGF induces NF-κB activation in a variety of tumors, such as breast, colon, non-small cell lung, and pancreatic cancers (34-37). To verify EGF-induced NF-κB activation in RCC cells, a previous study treated tumor cells with 10 ng/ml EGF (38). The results showed a time-dependent decrease in IκB content and increasing p-p65/p65 content. Therefore, it can be concluded that EGF induces NF-κB activation in RCC cells. To further demonstrate the ability of CARD10 to mediate EGF-induced NF-κB activation, CARD10 shRNA-transfected RCC cells were treated with EGF. The results showed a significant decrease in NF-κB activation in the shRNA-transfected group compared with that in the negative control group at the same time point. As the expression of CARD10 in RCC is higher than that in normal renal tubular epithelial cells, the activation of the NF-κB signaling pathway was further analyzed with the prolongation of EGF treatment time. The results showed that NF-κB activation in RCC cell lines was significantly higher than that in normal renal tubular epithelial cells. Therefore, it was concluded that CARD10 mediates NF-κB activation in RCC cells.

In conclusion, the expression of CARD10 was significantly increased in RCC cells. Furthermore, CARD10 promoted proliferation, invasion and migration of RCC cells, while also inhibiting the apoptosis of RCC cells via the regulation of the NF-κB signaling pathway. This study preliminarily explored the mechanism by which CARD10 regulates the development and progression of RCC. This information is important for the early diagnosis of RCC and the design of targeted therapy.

Acknowledgements

Funding

Availability of data and materials

The datasets used and/or analyzed during the current study are available from the corresponding author on reasonable request.

Authors' contributions

LP participated in the design of the study and analysis of data, and drafted the manuscript. LB and DY designed the study and drafted the manuscript. KH, ZC, JW and QW were involved in analysis and interpretation of data. Authors whose names appear on the submission have contributed sufficiently to the scientific work and therefore share collective responsibility and accountability for the results.

Ethics approval and consent to participate

Not applicable.

Patient consent for publication

Not applicable.

Competing interests

The authors declare that they have no competing interests.

References

1. Capitanio U and Montorsi F: Renal cancer. Lancet 387: 894-906, 2016.
2. Kuusk T, Grivas N, de Bruijn R and Bex A: The current management of renal cell carcinoma. Minerva Med 108: 357-369, 2017.
3. Gupta K, Miller JD, Li JZ, Russell MW and Charbonneau C: Epidemiologic and socioeconomic burden of metastatic renal cell carcinoma (mRCC): A literature review. Cancer Treat Rev 34: 193-205, 2008.
4. Zotti T, Polvere I, Voccola S, Vito P and Stilo R: CARD14/CARMA2 signaling and its role in inflammatory skin disorders. Front Immunol 9: 2167, 2018.
5. Scudiero I, Vito P and Stilo R: The three CARMA sisters: So different, so similar: A portrait of the three CARMA proteins and their involvement in human disorders. J Cell Physiol 229: 990-997, 2014.
6. Stilo R, Liguoro D, Di Jeso B, Formisano S, Consiglio E, Leonardi A and Vito P: Physical and functional interaction of CARMA1 and CARMA3 with Ikappa kinase gamma-NFkappaB essential modulator. J Biol Chem 279: 34323-34331, 2004.
7. Blonska M and Lin X: NF-κB signaling pathways regulated by CARMA family of scaffold proteins. Cell Res 21: 55-70, 2011.
8. Jiang C and Lin X: Regulation of NF-κB by the CARD proteins. Immunol Rev 246: 141-153, 2012.
9. Juilland M and Thome M: Holding all the CARDs: How MALT1 controls CARMA/CARD-dependent signaling. Front Immunol 9: 1927, 2018.
10. Wang L, Qian L, Li X and Yan J: MicroRNA-195 inhibits colorectal cancer cell proliferation, colony-formation and invasion through targeting CARMA3. Mol Med Rep 10: 473-478, 2014.
11. Chang YW, Chiu CF, Lee KY, Hong CC, Wang YY, Cheng CC, Jan YH, Huang MS, Hsiao M, Ma JT and Su JL: CARMA3 represses metastasis suppressor NME2 to promote lung cancer stemness and metastasis. Am J Respir Crit Care Med 192: 64-75, 2015.
12. Du S, Jia L, Zhang Y, Fang L, Zhang X and Fan Y: CARMA3 is upregulated in human pancreatic carcinoma, and its depletion inhibits tumor proliferation, migration, and invasion. Tumour Biol 35: 5965-5970, 2014.
13. Ekambaram P, Lee JL, Hubel NE, Hu D, Yerneni S, Campbell PG, Pollock N, Klei LR, Concel VJ, Delekta PC, *et al*: The CARMA3-Bcl10-MALT1 signalosome drives NFκB activation and promotes aggressiveness in angiotensin II receptor-positive breast cancer. Cancer Res 78: 1225-1240, 2018.

14. Xie C, Han Y, Fu L, Li Q, Qiu X and Wang E: Overexpression of CARMA3 is associated with advanced tumor stage, cell cycle progression, and cisplatin resistance in human epithelial ovarian cancer. Tumour Biol 35: 7957-7964, 2014.
15. Wu GL, Yuan JL, Huang XD, Rong JF, Zhang LX, Liu YP and Wang FL: Evaluating the expression of CARMA3 as a prognostic tumor marker in renal cell carcinoma. Tumour Biol 34: 3431-3435, 2013.
16. Zhang X, Liu X, Jing Z, Bi J, Li Z, Liu X, Li J, Li Z, Zhang Z and Kong C: The circINTS4/miR-146b/CARMA3 axis promotes tumorigenesis in bladder cancer. Cancer Gene Ther, 2019 (Epub ahead of print).
17. Man X, He J, Kong C, Zhu Y and Zhang Z: Clinical significance and biological roles of CARMA3 in human bladder carcinoma. Tumour Biol 35: 4131-4136, 2014.
18. Mahanivong C, Chen HM, Yee SW, Pan ZK, Dong Z and Huang S: Protein kinase C alpha-CARMA3 signaling axis links Ras to NF-kappa B for lysophosphatidic acid-induced urokinase plasminogen activator expression in ovarian cancer cells. Oncogene 27: 1273-1280, 2008.
19. Wang D, You Y, Lin PC, Xue L, Morris SW, Zeng H, Wen R and Lin X: Bcl10 plays a critical role in NF-kappaB activation induced by G protein-coupled receptors. Proc Natl Acad Sci USA 104: 145-150, 2007.
20. Zhang S, Zhang C, Liu W, Zheng W, Zhang Y, Wang S, Huang D, Liu X and Bai Z: MicroRNA-24 upregulation inhibits proliferation, metastasis and induces apoptosis in bladder cancer cells by targeting CARMA3. Int J Oncol 47: 1351-1360, 2015.
21. Senftleben U, Cao Y, Xiao G, Greten FR, Krähn G, Bonizzi G, Chen Y, Hu Y, Fong A, Sun SC and Karin M: Activation by IKKalpha of a second, evolutionary conserved, NF-kappa B signaling pathway. Science 293: 1495-1499, 2001.
22. Zhang S and Lin X: CARMA3: Scaffold protein involved in NF-κB signaling. Front Immunol 10: 176, 2019.
23. Mitchell S, Vargas J and Hoffmann A: Signaling via the NFκB system. Wiley Interdiscip Rev Syst Biol Med 8: 227-241, 2016.
24. Dolcet X, Llobet D, Pallares J and Matias-Guiu X: NF-kB in development and progression of human cancer. Virchows Arch 446: 475-482, 2005.
25. Cildir G, Low KC and Tergaonkar V: Noncanonical NF-κB signaling in health and disease. Trends Mol Med 22: 414-429, 2016.
26. DiDonato JA, Mercurio F and Karin M: NF-κB and the link between inflammation and cancer. Immunol Rev 246: 379-400, 2012.
27. Xia Y, Shen S and Verma IM: NF-κB, an active player in human cancers. Cancer Immunol Res 2: 823-830, 2014.
28. McAuley JR, Freeman TJ, Ekambaram P, Lucas PC and McAllister-Lucas LM: CARMA3 is a critical mediator of G protein-coupled receptor and receptor tyrosine kinase-driven solid tumor pathogenesis. Front Immunol 9: 1887, 2018.
29. Jiang C and Lin X: Analysis of epidermal growth factor-induced NF-κB signaling. Methods Mol Biol 1280: 75-102, 2015.
30. Pan D and Lin X: Epithelial growth factor receptor-activated nuclear factor κB signaling and its role in epithelial growth factor receptor-associated tumors. Cancer J 19: 461-467, 2013.
31. Pan D, Zhu Y, Zhou Z, Wang T, You H, Jiang C and Lin X: The CBM complex underwrites NF-κB activation to promote HER2-associated tumor malignancy. Mol Cancer Res 14: 93-102, 2016.
32. Jiang C, Zhou Z, Quan Y, Zhang S, Wang T, Zhao X, Morrison C, Heise MT, He W, Miller MS and Lin X: CARMA3 is a host factor regulating the balance of inflammatory and antiviral responses against viral infection. Cell Rep 14: 2389-2401, 2016.
33. Chen R, Jin G and McIntyre TM: The soluble protease ADAMDEC1 released from activated platelets hydrolyzes platelet membrane pro-epidermal growth factor (EGF) to active high-molecular-weight EGF. J Biol Chem 292: 10112-10122, 2017.
34. Elbaz M, Nasser MW, Ravi J, Wani NA, Ahirwar DK, Zhao H, Oghumu S, Satoskar AR, Shilo K, Carson WE III and Ganju RK: Modulation of the tumor microenvironment and inhibition of EGF/EGFR pathway: Novel anti-tumor mechanisms of Cannabidiol in breast cancer. Mol Oncol 9: 906-919, 2015.
35. Li Y, Lin Z, Chen B, Chen S, Jiang Z, Zhou T, Hou Z and Wang Y: Ezrin/NF-kB activation regulates epithelial-mesenchymal transition induced by EGF and promotes metastasis of colorectal cancer. Biomed Pharmacother 92: 140-148, 2017.
36. Wu W, Jaspers I, Zhang W, Graves LM and Samet JM: Role of Ras in metal-induced EGF receptor signaling and NF-kappaB activation in human airway epithelial cells. Am J Physiol Lung Cell Mol Physiol 282: L1040-L1048, 2002.
37. Liptay S, Weber CK, Ludwig L, Wagner M, Adler G and Schmid RM: Mitogenic and antiapoptotic role of constitutive NF-kappaB/Rel activity in pancreatic cancer. Int J Cancer 105: 735-746, 2003.
38. Jiang T, Grabiner B, Zhu Y, Jiang C, Li H, You Y, Lang J, Hung MC and Lin X: CARMA3 is crucial for EGFR-Induced activation of NF-κB and tumor progression. Cancer Res 71: 2183-2192, 2011.